JEM

Supplemental material

Chen et al., https://doi.org/10.1084/jem.20171849

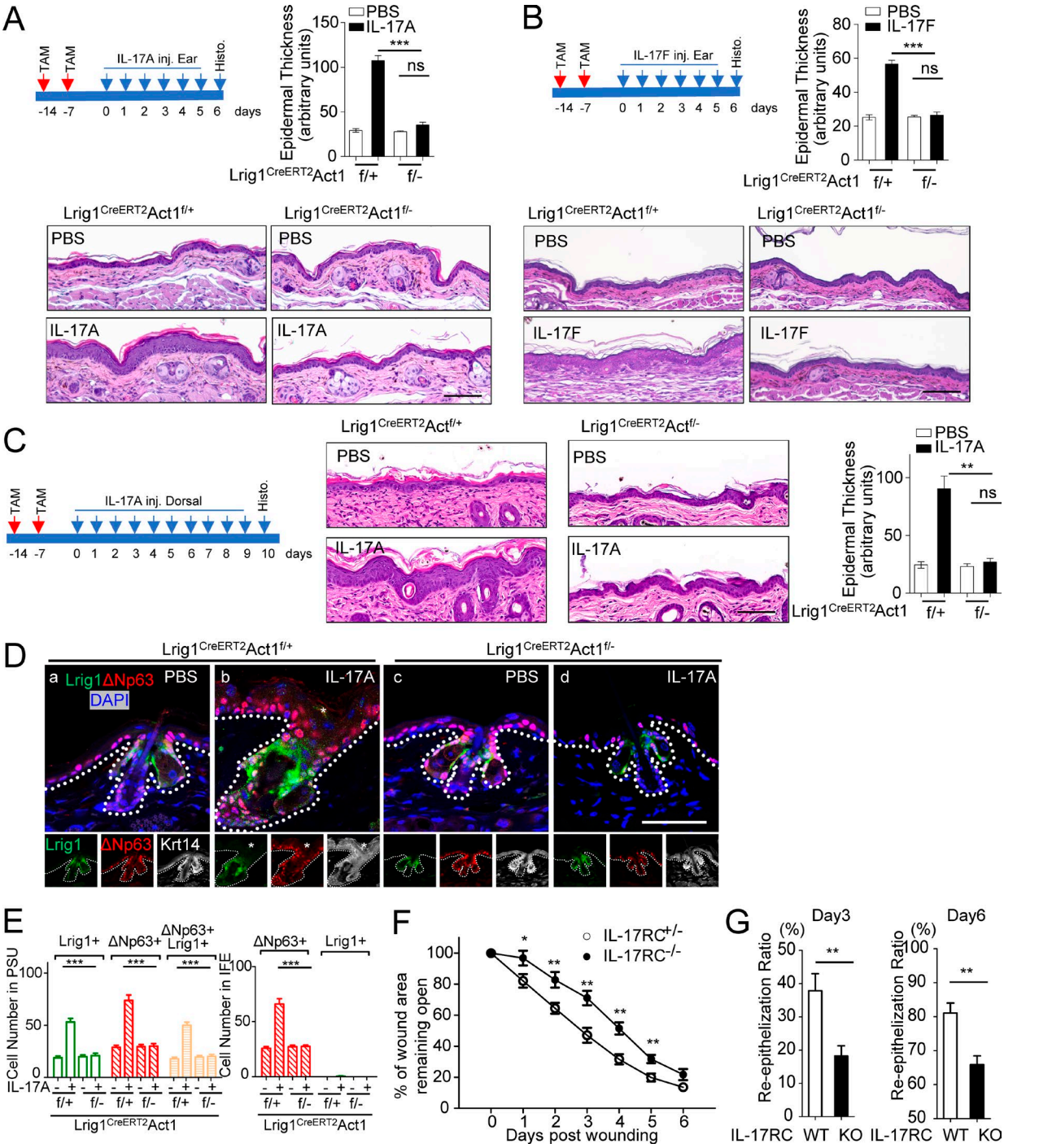

Figure S1. **IL-17A–induced signaling in epidermal hyperplasia and wound healing. (A and B)** H&E staining of ear skin tissue from Lrig^{CreERT2}Act1$^{f/+}$ and Lrig1^{CreERT2}Act1$^{f/-}$ mice injected intradermally with IL-17A (500 ng; A), IL-17F (1 µg; B), or PBS daily for 6 consecutive d. Mice were intraperitoneally injected with two doses of tamoxifen (~5 mg/25 g weight) 14 and 7 d before IL-17A (A) or IL-17F (B) injection. *n* = 5 per group. Graph shows mean epidermal thickness (arbitrary units) ± SEM (five fields were analyzed; ***, P < 0.001; ns, not significant, *t* test). Bar, 100 µm. TAM, tamoxifen. **(C)** H&E staining of dorsal skin from of Lrig^{CreERT2}Act1$^{f/+}$ and Lrig1^{CreERT2}Act1$^{f/-}$ mice that were subjected to multispot dorsal intradermal injection of with IL-17A (1.25 µg each spot, six spots) or PBS daily for 10 consecutive d. Mice were injected with two doses of tamoxifen (~5 mg/25 g weight) 14 and 7 d before IL-17A injection. Graph presents mean epidermal thickness (arbitrary units) ± SEM (five fields were analyzed; **, P < 0.001, *t* test). Bars, 100 µm. Data are representative of three independent experiments shown in A–C. **(D)** Sections of PBS (a and c) and IL-17A–injected ears (b and d; day 6) of indicated genotypes from Fig. 1 A were stained for Lrig1^{+} (green) and ΔNp63 (red). The asterisk indicates nonspecific staining of the stratum corneum. **(E)** Quantification of Lrig1^{+}, ΔNp63^{+}, and Lrig1^{+}ΔNp63^{+} in 10 PSUs and adjacent IFE. *n* = 5 mice per group. Bar graphs show ± SEM. ***, P < 0.001, *t* test. Bars, 50 µm. Data are representative of three independent experiments. **(F)** Wound-closure kinetics in IL-17RC$^{+/-}$ and littermate IL-17RC$^{-/-}$ mice. Graph represents the percentage of wound area remaining open ± SEM from four mice. *, P < 0.01; **, P < 0.05, *t* test. Data are representative of three independent experiments. **(G)** Measurement of reepithelization ratio (leading edge ratio) in wound area at day 6 of IL-17RC$^{+/-}$ (WT) and littermate IL-17RC$^{-/-}$ (KO) mice, ± SEM from 3 sections of each wound and total 10 wounds. **, P < 0.01, *t* test. Data are representative of three independent experiments.

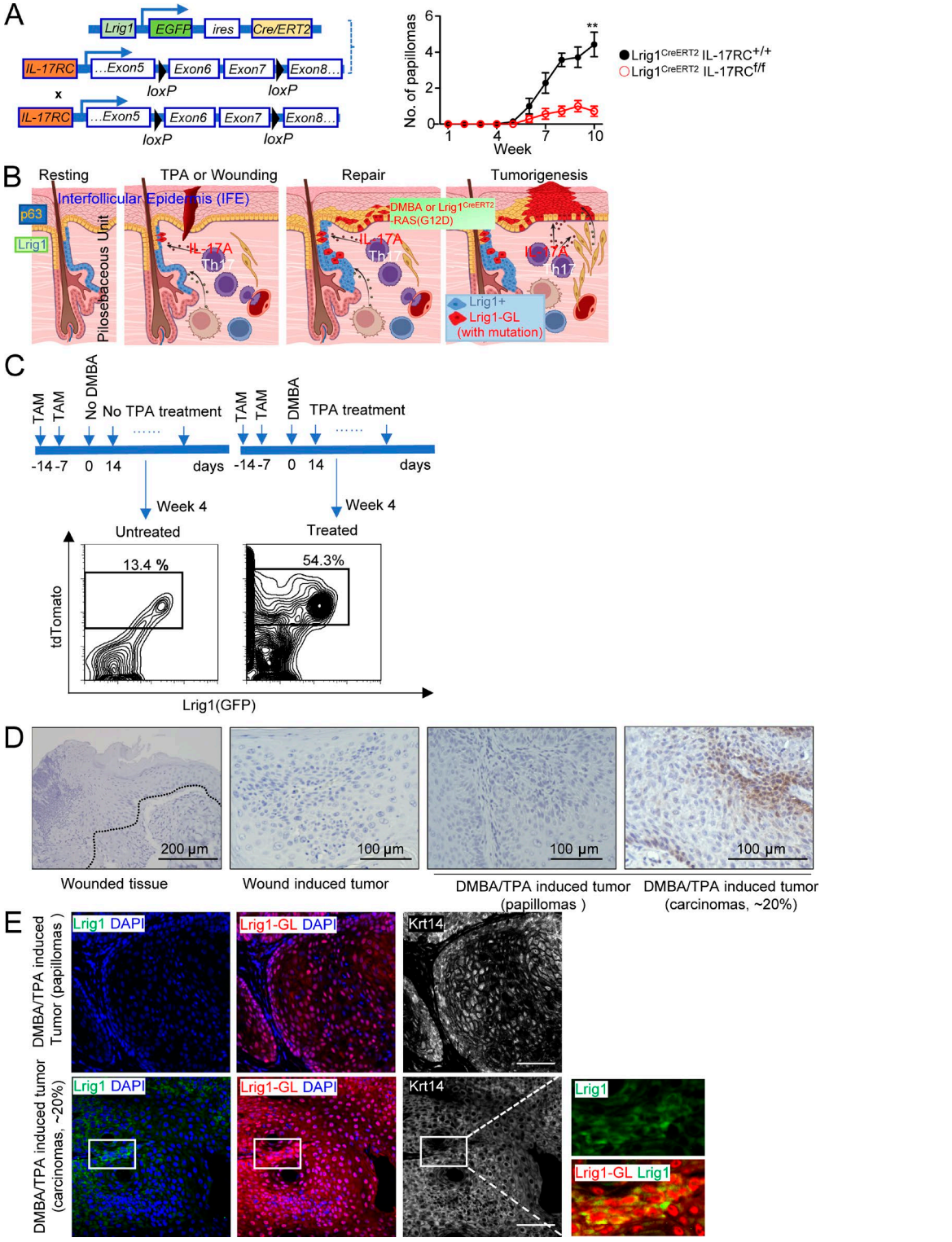

Figure S2. **IL-17A–induced signaling in Lrig1⁺ cells drives Lrig1 progenies to participate in skin tumorigenesis. (A)** DMBA/TPA-induced tumor/papilloma numbers in Lrig1^{CreERT2}IL-17RC$^{+/+}$ and Lrig1^{CreERT2}IL-17RC$^{f/f}$ mice. Mice were injected with tamoxifen (~5 mg/25 g weight) 7 and 14 d before DMBA/TPA treatment. *n* = 7 per group. The data are presented as average tumor numbers per mouse ± SEM. **, P < 0.01, *t* test. Data are representative of two independent experiments. Lrig1^{CreERT2}/IL-17RC$^{f/f}$ mice were obtained after at least eight generations of breeding. **(B)** Model for IL-17A–dependent wound healing and skin tumorigenesis. **(C)** Epidermal cells from DMBA/TPA-treated dorsal skin were analyzed by flow cytometry for GFP and tdTomato. Data are representative of two independent experiments. TAM, tamoxifen. **(D)** Paraffin sections of the wound tissue, wound-induced tumors (Fig. 3 A), and DMBA/TPA-induced tumor were subjected to DAB staining for Lrig1 (AF3688; R&D Systems). **(E)** Lineage tracing showed that Lrig1-GL cells (anti-tdTomato; red) were costained as Lrig1 (AF3688; R&D Systems; in ~20% tumor tissue induced by the DMBA/TPA model; Fig. 3 K). The epithelial border was indicated by Krt14 staining. Bars, 50 μm. For D and E, data are representative of at least five specimens for each experiment and were verified in three independent experiments.

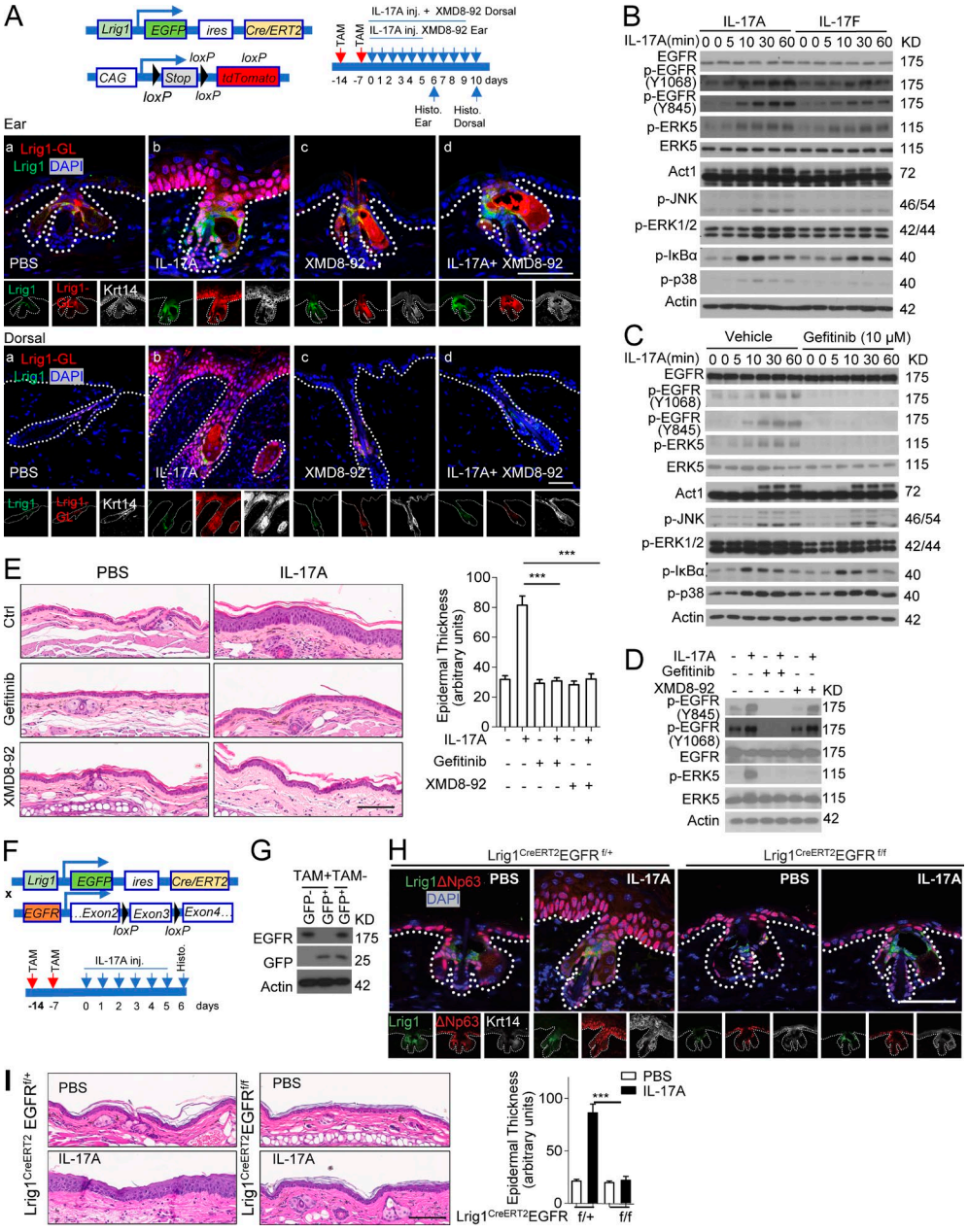

Figure S3. **IL-17A–induced EGFR activation in Lrig1⁺ stem cells is required for the migration and expansion of Lrig1 progenies. (A)** Lrig1^{CreERT2} mice in ROSA26-LSL-tdTomato background were injected with two doses of tamoxifen (~5 mg/25 g weight) before IL-17A injection. Ear skin or dorsal skin were intradermally injected with PBS and IL-17A (500 ng) combined with XMD8-92 (20 µl of 5 µM) daily as indicated. Skin sections were used to show Lrig1⁺ (GFP; green) and migration of Lrig1⁺ progenies (Lrig1-GL, tdTomato; red) to the epidermis. Bars, 50 µm. Data are representative from at least five mice for each experiment and were verified in two independent experiments. **(B)** Keratinocytes isolated from WT mice were stimulated with 100 ng/ml IL-17A or 200 ng/ml IL-17F for the indicated times, followed by Western blot analyses with the indicated antibodies. **(C)** Primary keratinocytes with and without pretreatment of EGFR inhibitor (gefitinib, 10 µM; 30 min) were stimulated with IL-17A followed by Western blot analyses with the indicated antibodies. Data are representative of three independent experiments. **(D)** Western blot analysis of epidermal lysates from WT mice injected with IL-17A with or without gefitinib (20 µl of 10 µM) and XMD8-92 (20 µl of 5 µM) for 30 min. Lysates were homogenized from ear skin samples from three female C57/B6 mice per group. Data are representative of three independent experiments. **(E)** H&E staining of ear sections from WT mice injected intradermally with PBS and IL-17A (500 ng) combined with gefitinib (20 µl of 10 µM) or XMD8-92 (20 µl of 5 µM) daily for 6 consecutive d; *n* = 5 mice each group. Graph presents mean epidermal thickness (arbitrary units; five fields were analyzed, ± SEM; ***, P < 0.001, *t* test). Bars, 100 µm. Data are representative of three independent experiments. **(F)** Schematic representation of the genetic elements for Lrig1 reporter, EGFR deletion and the experimental setup for G–I. Lrig1^{CreERT2} EGFR$^{f/+}$ and Lrig1^{CreERT2}EGFR1$^{f/f}$ littermate mice were intraperitoneally injected with tamoxifen (~5 mg/25 g weight) before intradermal IL-17A injection. IL-17A (500 ng) or PBS were injected daily for 6 consecutive d. **(G)** Western blot analysis of flow cytometry–sorted epidermal cells from Lrig1^{CreERT2}EGFR1$^{f/f}$ mice before IL-17A injection (day 0) as shown in F. **(H)** Sections of PBS- and IL-17A-injected ears (day 6) of indicated littermate mice were analyzed for Lrig1 (green) and ΔNp63 (red). Representative PSU and adjacent IFE are shown. Five mice were analyzed for each genotype. Data are representative of three independent experiments. **(I)** H&E staining of ear skin tissue from F and G. *n* = 5 per group. Graph presents mean epidermal thickness (arbitrary units; five fields were analyzed; Error bars represent ± SEM; ***, P < 0.001; ns, not significant, *t* test). Bar, 100 µm. Data are representative of three independent experiments.

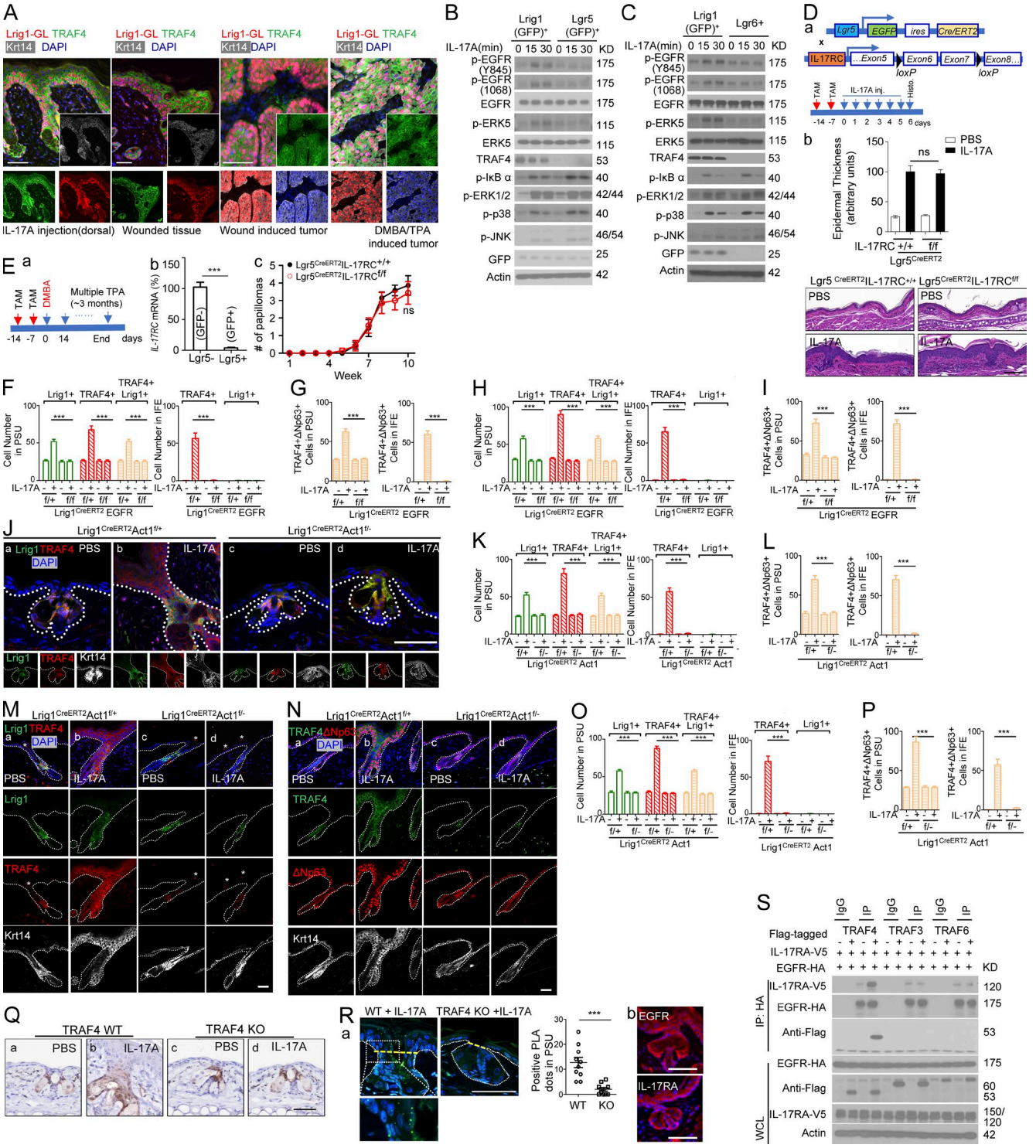

Figure S4. **TRAF4 is enriched in Lrig1⁺ stem cells and required for IL-17A–induced IL-17RA–EGFR interaction. (A)** Paraffin sections of the IL-17A–injected dorsal skin (day 10), wound tissue (day 3), wound-induced tumors, and DMBA/TPA-induced tumor were subjected to staining for Lrig1-GL(tdTomato) and TRAF4. Bars, 50 µm. Data are representative of at least five specimens for each experiment and were verified in three independent experiments. **(B)** Primary Lrig1(GFP)⁺ and Lgr5(GFP)⁺ keratinocytes from Lrig1^{CreERT2} and Lgr5 ^{CreERT2} reporter mice were isolated and sorted by FACS, followed by 100 ng/ml IL-17A stimulation and Western blot analyses with the indicated antibodies. **(C)** Primary Lrig1(GFP)⁺ and Lgr6⁺ keratinocytes from Lrig1^{CreERT2} reporter mice were isolated and sorted by FACS, followed by 100 ng/ml IL-17A stimulation and Western blot analyses with the indicated antibodies. Data are representative of three independent experiments shown in B and C. **(D)** Schematic representation of the genetic elements for Lgr5 reporter, IL-17RC deletion, and the experimental setup (a). Lgr5^{CreERT2}IL-17RC$^{+/+}$and Lgr5^{CreERT2}IL-17RC$^{f/f}$ littermate mice were intraperitoneally injected with tamoxifen (~5 mg/25 g weight) before intradermal IL-17A injection. IL-17A (500 ng) or PBS were injected daily for 6 consecutive d. H&E staining of ear skin tissue (b). Graph presents mean epidermal thickness (arbitrary units) ± SEM (five fields were analyzed; ns, not significant, *t* test). Bar, 100 µm. Data are representative of three independent experiments. TAM, tamoxifen. **(E)** DMBA/TPA-induced tumor/papilloma numbers in Lgr5^{CreERT2}IL-17RC$^{+/+}$ and Lgr5^{CreERT2}IL-17RC$^{f/f}$ mice. Mice were injected with

tamoxifen (~5 mg/25 g weight) 7 and 14 d before DMBA/TPA treatment (a). IL-17RC deletion in Lgr5$^+$ cell was determined by qPCR analysis of *IL-17RC* mRNA level in flow cytometry–sorted epidermal cells from Lgr5^{CreERT2}IL-17RC$^{f/f}$ littermate mice before DMBA application (day 0; b) as shown in a. Primers targeting *IL-17RC* mRNA sequence encoding Exon 6–7 were used. Forward, 5′-GTTTCGAGGCTAGTCTTGGGG-3′; reverse, 5′-GAGCTCTTTCTGGTACCTGGG-3′. Graph presents relative mRNA change ± SEM from three biological replicates. ***, P < 0.001, *t* test. The data are presented as average tumors numbers per mice ± SEM (c). *n* = 7 per group. ns, not significant, *t* test. Data are representative of two independent experiments. **(F and G)** Quantification of Lrig1$^+$, TRAF4$^+$, Lrig1$^+$ TRAF4$^+$, or TRAF4$^+$ΔNp63$^+$ in the PSU and IFE for the data presented in Fig. 6 D (a–d) and Fig. 6 E (a–d). **(H and I)** Quantification of Lrig1$^+$, TRAF4$^+$, Lrig1$^+$ TRAF4$^+$, or TRAF4$^+$ΔNp63$^+$ in the PSU and IFE for the data presented in Fig. 6 D (e–h) and Fig. 6 E (e–h). For F–I, 10 PSUs and adjacent IFE were analyzed. Five mice were analyzed for each genotype (±SEM; ***, P < 0.001, *t* test). Data are representative of three independent experiments. **(J)** Paraffin sections described in Fig. S1 D (a–d) were subjected to double staining of Lrig1 (anti-GFP; green) and TRAF4 (red; a–d). Bars, 50 µm. **(K)** Quantification of Lrig1$^+$, TRAF4$^+$, and Lrig1$^+$ TRAF4$^+$ in the PSU and IFE for the data presented in J (10 PSUs and adjacent IFE were analyzed; ±SEM; ***, P < 0.001, *t* test). **(L)** Quantification of TRAF4$^+$ΔNp63$^+$ from paraffin section staining described in Fig. S1 D (a–d; 10 PSUs and adjacent IFE were analyzed each section; ±SEM; ***, P < 0.001, *t* test). **(M–P)** Dorsal skin sections from indicated littermate mice were stained for Lrig1 (GFP; green) and TRAF4 (red; M, a–d) or TRAF4 (green) and p63 (ΔNp63; red; N, a–d). Bars, 50 µm. The asterisk indicates nonspecific staining of the stratum corneum. 10 PSUs and adjacent IFE were analyzed for O and P. ±SEM; ***, P < 0.001, *t* test. Five mice were analyzed for each genotype. Data are representative of three independent experiments. **(Q)** Ear skin sections from TRAF4$^{+/+}$ and TRAF4$^{-/-}$ littermate mice injected with PBS (a and c) or IL-17A (500 ng; b and d) daily for 6 consecutive d were subjected to staining of Lrig1 (AF3688; R&D). Data are representative from at least five mice for each experiment and were verified in three independent experiments. **(R)** Ear skin sections from TRAF4 WT and TRAF4 KO littermate mice injected with IL-17A (500 ng) daily for 6 consecutive d were subjected to PLA (a). Mouse anti-EGFR (Thermo Fisher Scientific) and rabbit anti–IL-17RA antibodies (Covance) were used for the assay. Green dots present the interaction between EGFR and IL-17RA. Graph represents mean of positive dots from 10 PSUs (outlined by yellow dashed line). ±SEM; ***, P < 0.001, *t* test. Bar, 50 µm. Data are representative of three independent experiments. Immunofluorescence staining of ear skin tissue for EGFR and IL-17RA with the antibodies used in the PLA (b). Monovalent Fab fragment of donkey anti-mouse IgG was used to block endogenous IgG before EGFR antibody incubation. Bar, 50 µm. **(S)** Flag-tagged TRAF4, TRAF3, or TRAF6 were cotransfected with V5-tagged IL-17RA and HA-tagged EGFR into HeLa cells. Cell lysates were immunoprecipitated with mouse anti-HA (EGFR), followed by Western blot analyses with the indicated antibodies. Data are representative of three independent experiments. WCL, whole cell lysate; IP, immunoprecipitation.

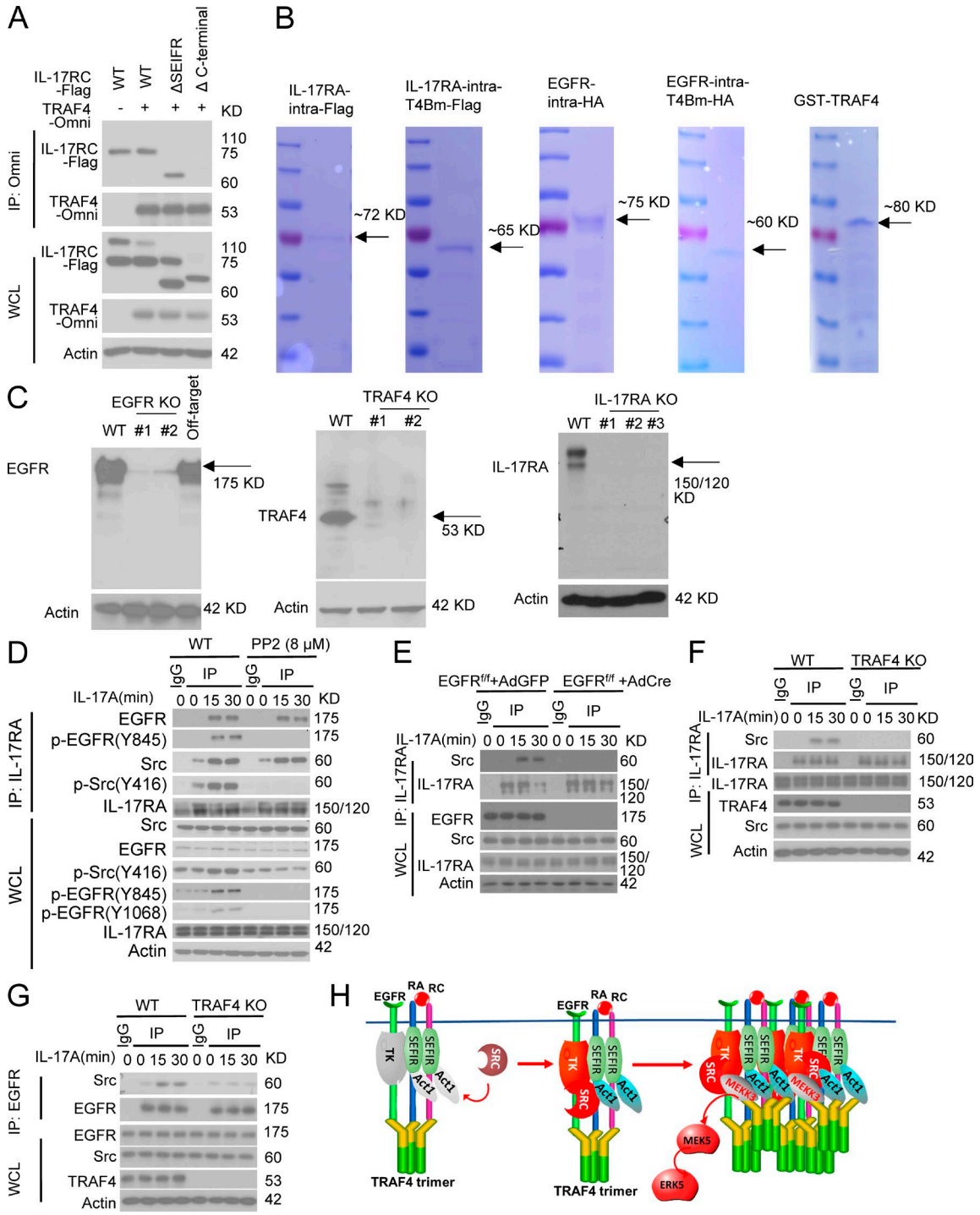

Figure S5. **IL-17R–EGFR transactivation. (A)** Omni-tagged TRAF4 was cotransfected with the indicated Flag-tagged IL-17RC mutants into IL-17RA KO HeLa cells. Cell lysates were immunoprecipitated with anti-Omni (TRAF4), followed by Western blot analysis. Data are representative of at least three experiments. **(B)** Coomassie blue staining of SDS-PAGE resolved recombinant IL-17RA and EGFR protein used in Fig. 8 (K and L). **(C)** Western analysis of EGFR, IL-17RA, and TRAF4 KO clones derived from HeLa cells. Rabbit anti-EGFR (Abcam), rabbit anti-human IL-17RA (Cell Signaling Technology), and goat anti-TRAF4 (Santa Cruz Biotechnology) antibodies were used. Data were verified in three independent experiments. **(D)** Primary keratinocytes with and without pretreatment of Src inhibitor (PP2, 8 μM; 30 min) were then treated with 100 ng/ml IL-17A for the indicated times. Cell lysates were then immunoprecipitated with anti-mouse–IL-17RA followed by Western blot analysis with the indicated antibodies. **(E)** Primary keratinocytes were isolated from EGFR$^{f/f}$ mice, followed by infection with adenovirus containing Cre-recombinase (AdCre) or empty vector (AdGFP). Cell lysates were then immunoprecipitated with anti-mouse–IL-17RA followed by Western blot analysis with the indicated antibodies. **(F and G)** Primary keratinocytes were isolated from TRAF4 WT and TRAF4 KO littermate mice. Cell lysates were then immunoprecipitated with anti-mouse–IL-17RA (F) and anti-EGFR (G) followed by Western analysis with the indicated antibodies. For D–G, data are representative of at least three experiments. WCL, whole cell lysate; IP, immunoprecipitation. **(H)** Model for IL-17R-EGFR–induced ERK5 activation. In response to IL-17A stimulation, TRAF4 tethers IL-17R and EGFR, which allows Act1 to recruit c-Src to the IL-17R–EGFR complex. The activated c-Src mediates EGFR transactivation followed by downstream activation of MEKK3-ERK5.

Table S1. **Key antibodies and reagents**

Antibodies and reagents	Source	Identifier
Rat anti-humanAct1	eBioscience (1:1,000 for WB)	Cat. no. 14-4040-80, Clone: 9ACT12
Rabbit anti-mouseAct1	(1:2,000 for WB)	Zhang et al., 2014
Rabbit anti-Act1	Santa Cruz Biotechnology (1:200 for IP)	Cat. no. sc-11444
Mouse anti-Flag tag	Sigma-Aldrich (1:150 for staining; 1: 3,000 for WB)	Cat. no. F3165
Rabbit anti-Flag tag	Cell Signaling Technology (1:150 for staining; 1:1,000 for WB)	Cat. no. 14793
Mouse anti-HA tag	Sigma-Aldrich (1:150 for staining; 1:3,000 for WB)	Cat. no. H9658
Rabbit anti-HA tag	Cell Signaling Technology (1:150 for staining; 1:1,000 for WB)	Cat. no. 3724
Rabbit anti-myc tag	Cell Signaling Technology (1:150 for staining)	Cat. no. 2278
Mouse anti-V5 tag	Thermo Fisher Scientific (1:500 for IP)	Cat. no. R960-25
Rabbit anti-V5 tag	Cell Signaling Technology (1:1,000 for WB)	Cat. no. 13202
Mouse anti-Omni-tag	Santa Cruz Biotechnology (1:1,000 for WB)	Cat. no. sc-7270
Rabbit anti-Omni-tag	Santa Cruz Biotechnology (1:1,000 for WB; 1 µg/ml for IP)	Cat. no. sc-499
Rabbit anti-ΔNp63	BioLegend (1:300 for staining)	Cat. no. 619001
Rabbit anti-GFP	Cell Signaling Technology (1:100 for staining, 1:1,000 for WB)	Cat. no. 2956
Mouse anti-GFP	Cell Signaling Technology (1:100 for staining)	Cat. no. 2955
Cytokeratin 14 Antibody (LL002) Alexa Fluor 647	Santa Cruz Biotechnology (1:50 for staining)	Cat. no. sc-58724 AF647
Rat anti-tdTomato	Kerafast (1:100 for staining)	Cat. no. EST203
Rabbit anti-tdTomato (labeled with Thermo Alexa Fluor 568 Antibody Labeling Kit)	Rockland	Cat. no. 600-401-379
Rabbit anti-Ki67	Abcam (1:150 for staining)	Cat. no. ab15580
Rabbit anti-Krt14	Biolegend (1:1,000 for staining)	Cat. no. PRB-155P
Goat anti-TRAF4	Santa Cruz Biotechnology (1:250 for staining)	Cat. no. sc-1920
Rabbit anti-EGFR	Bethyl Laboratories (1:300 for staining)	Cat. no. IHC-00005
Rabbit anti-EGFR	Abcam (1:1,000 for WB; 1:200 for IP)	Cat. no. ab52894
Mouse anti-EGFR	Thermo Fisher Scientific (1:50 for in situ PLA assay)	MA5-13070, Clone H11
Rabbit anti-KrasG12D	Cell Signaling Technology (1:1,000 for WB)	Cat. no. 14429
Rabbit anti-Kras	Cell Signaling Technology (1:1,000 for WB)	Cat. no. 8955
Rabbit anti-pEGFR (Y845)	Cell Signaling Technology (1:1,000 for WB)	Cat. no. 6963
Rabbit anti-pEGFR (Y1068)	Cell Signaling Technology (1:1,000 for WB)	Cat. no. 3777
Rabbit anti-pSrc (Y416)	Cell Signaling Technology (1:1,000 for WB)	Cat. no. 6943
Rabbit anti-Src	Cell Signaling Technology (1:1,000 for WB)	Cat. no. 2108
Rabbit anti-pp38	Cell Signaling Technology (1:1,000 for WB)	Cat. no. 9211
Rabbit anti-pJNK	Cell Signaling Technology (1:1,000 for WB)	Cat. no. 9251
Mouse anti-pERK1/2	Santa Cruz Biotechnology (1:1,000 for WB)	Cat. no. sc-7383
Goat anti-mouse Lrig1	R&D Systems (10 µg/ml for staining)	Cat. no. AF3688
Rabbit anti-Lgr6	Proteintech (0.4 µg per million cells)	Cat. no. 17658-1-AP
Mouse anti-Phosphotyrosine	EMD Millipore (1:1,000 for WB)	Cat. no. 05-321, Clone 4G10
Mouse anti-MEKK3	BD Biosciences (1:200 for IP)	Cat. no. 611102, Clone 40
Rabbit anti-pIκBα	Cell Signaling Technology (1:1,000 for WB)	Cat. no. 2859
Rabbit anti-ERK5	Cell Signaling Technology (1:1,000 for WB)	Cat. no. 3372
Rabbit anti-IL-17RA (human only)	Cell Signaling Technology (1:1,000 for WB)	Cat. no. 12661
Rabbit-anti-CD34	Abcam (1:100 for IF)	Cat. no. Ab81289
Rabbit anti-Sox2	Abcam (1:100 for IF)	Cat. no. Ab92494
Goat anti-Actin	Santa Cruz Biotechnology (1:1,000 for WB)	Cat. no. sc-1615

Table S1. **Key antibodies and reagents *(Continued)***

Antibodies and reagents	Source	Identifier
Mouse anti-Actin	Cell Signaling Technology (1:5,000 for WB)	Cat. no. 3700
Anti-Rabbit IgG HRP- TrueBlot	Rockland Immunochemicals (1:2,000 for WB after IP)	Cat. no. 18-8816-31
Anti-Mouse IgG HRP-TrueBlot	Rockland Immunochemicals I (1:2,000 for WB after IP)	Cat. no. 18-8817-31
Goat Anti-Mouse IgG, Light Chain HRP	Jackson ImmunoResearch (1:5,000 for WB after IP)	Cat. no. 115-035-174
Mouse Anti-Rabbit IgG, Light Chain HRP	Jackson ImmunoResearch (1:5,000 for WB after IP)	Cat. no. 211-032-171
TPA	LC Laboratories	Cat. no. P-1680
DMBA	Sigma-Aldrich	Cat. no. D3254
Tamoxifen	Sigma-Aldrich	Cat. no. T5648
4-hydroxytamoxifen	Sigma-Aldrich	Cat. no. H7904
pp2	Sigma-Aldrich	Cat. no. 529573
Gefitinib	Selleck	Cat. no. S1025
XMD8-92	Apexbio	Cat. no. A3943
mIL-17A (in vitro cell culture)	R&D Systems	Cat. no. 421-ML
mIL-17A (in vivo)	R&D Systems	Cat. no. 421-ML/CF
mIL-17F (in vitro cell culture)	R&D Systems	Cat. no. 2057-IL
mIL-17F (in vivo)	R&D Systems	Cat. no. 2057-IL/CF
hIL-17A (in vitro cell culture)	R&D Systems	Cat. no. 317-ILB
Doxycycline	Sigma-Aldrich	Cat. no. D9891
Protease Inhibitor Cocktail	Sigma-Aldrich (from Roche)	Cat. no. 11836170001
Proximity ligation (Duolink) assay (Green)	Duolink in situ Green kit (Sigma-Aldrich)	Cat. no. DUO92014
Proximity ligation (Duolink) assay (Red)	Duolink in situ Red kit (Sigma-Aldrich)	Cat. no. DUO92008
HeLa	ATCC	Cat. no. CCL-2
293FT Packaging Cells	Thermo Fisher Scientific	Cat. no. R70007
Phoenix Packaging Cells	ATCC	Cat. no. CRL-3213
Ad-Cre-GFP Adenovirus	Vector Laboratories	Cat. no. 1700
Ad-GFP Adenovirus	Vector Laboratories	Cat. no. 1060
Rosetta (DE3) Competent Cells	EMD Millipore	Cat. no. 70954

WB, Western blot; IP, immunoprecipitation; IF, immunofluorescence.

References

Zhang, B., C. Liu, W. Qian, Y. Han, X. Li, and J. Deng. 2014. Structure of the unique SEFIR domain from human interleukin 17 receptor A reveals a composite ligand-binding site containing a conserved α-helix for Act1 binding and IL-17 signaling. *Acta Crystallogr. D Biol. Crystallogr.* 70:1476–1483. https://doi.org/10.1107/S1399004714005227